RSC
Mechanochemistry

ROYAL SOCIETY
OF **CHEMISTRY**

PAPER
Jose M. Palomo *et al.*
Mechanochemical synthesis of Zn-bionanohybrids: size
effect at the nanoscale to improve their enzyme-like activity

PAPER

Mechanochemical synthesis of Zn-bionanohybrids: size effect at the nanoscale to improve their enzyme-like activity†

Carla Garcia-Sanz, [ID] [a] Laura Guijarro,[a] Mirosława Pawlyta [ID] [b] and Jose M. Palomo [ID] *[a]

The mechanochemical synthesis of nanomaterials for catalytic applications is a growing research field owing to its simplicity, scalability, and eco-friendliness. In this work, we synthesised new zinc bionanohybrids *via* a mechanochemical method involving a size effect at the nanoscale and microscale levels of the final nanostructure. This effect translates into an improvement in the catalytic properties of this nanomaterial, such as enzyme-like activities, compared to that synthesized in an aqueous media. One-pot synthesis was performed by combining *Candida antarctica* lipase B (CALB) solution, solid zinc salts and phosphate or bicarbonate salts using the ball-milling approach, where overall reaction times were drastically reduced in comparison with the traditional aqueous method. The reaction was carried out at r.t. and the synthesis process was evaluated by considering the use of steel balls with different sizes, completely dry conditions or in the presence of a very small amount of water as an additive (2 mL), and incubation methods (planetary or horizontal ball milling). The final nanostructure of the Zn biohybrids was determined using XRD, FT-IR, TEM and SEM analysis, demonstrating changes in metal species and drastic changes in the nanostructure conformation of the biohybrids obtained through the mechanical approach compared to those obtained through the aqueous method. The size effect at the nanoscale was also demonstrated in the final species, showing a reduced size. This nanoscale effect of the material had a positive impact on the catalytic properties of the materials, in some cases showing up to 2000 times greater activity compared to the counterpart synthesised under aqueous conditions.

Introduction

The synthesis of transition metal nanoparticles (MeNPs) has been of great interest for applications in biomedicine, biotechnology and catalytic chemical synthesis.[1–3] Among the different strategies, a new type of nanostructured multi-metal catalytic system based on the creation of heterogeneous bio-hybrids of enzymes and metal nanoparticles in aqueous media has recently been developed. These biohybrids have been successfully applied in different types of reactions (oxidation, reduction, dynamic kinetic resolutions, cascade reactions, C–C, C–H reactions, *etc.*).[4–7] This new, innovative and efficient method represents a highly environmentally friendly way of obtaining them compared to other methods previously described in literature.[8,9] The enzyme plays a key role in this technology as it not only acts as a stabiliser, but also has the ability to induce the formation of these metallic nanoparticles *in situ* on the protein matrix, giving rise to so-called bionano-hybrids.[10] The enzyme is used as a scaffold to create the nanoparticles and keep them homogeneously dispersed and avoid aggregation. This technique also allows the size of the nanoparticles to be controlled, which is a critical factor in achieving high catalytic activity.[11,12]

In particular, the synthesis of Zn catalysts has attracted great interest owing to its high abundance in the earth's crust (0.0076%), affordability, and non-toxicity.[13] Surprisingly, the interest in zinc as a catalyst has been underdeveloped, but recently this situation has changed,[14] and the potential of zinc has been demonstrated in several applications such as C–C, C–N and C–O bond formation reactions[15–17] and in solid surface reactions such as acylation of alcohols, phenols and amines.[18,19]

Therefore, the development of methods for the synthesis of highly active, selective, stable and robust zinc nanoparticles (ZnNPs) is of great interest. Sustainable and cost-effective systems to produce large quantities of ZnNPs are also desirable from an application point of view. In terms of catalysis, zinc species are one of the most important moieties influencing the final properties of nanocatalysts.[20] However, in most cases,

[a] Instituto de Catálisis y Petroleoquímica (ICP), CSIC, c/Marie Curie 2, Campus UAM Cantoblanco, 28049 Madrid, Spain. E-mail: josempalomo@icp.csic.es

[b] Faculty of Mechanical Technology, Silesian Technical University, Stanisława Konarskiego 18A, 44-100 Gliwice, Poland

† Electronic supplementary information (ESI) available: TEM figures, XRD pattern, ICP-OES analysis results. See DOI: https://doi.org/10.1039/d4mr00019f

it takes a long time to synthesise these catalysts and give rise to large structures with low catalytic activity.[21,22]

To overcome these shortcomings, mechanochemistry has been applied successfully to the synthesis of enzyme-MeNPs systems.[23] Mechanochemistry[24,25] - chemical synthesis enabled or supported by mechanical force – is undergoing an exciting period of rediscovery thanks to new synthetic methods and tools for real-time mechanistic research, and has been identified by IUPAC as one of the 10 world-changing technologies.[26–29] In particular, ball milling has emerged in recent years as an excellent green chemistry method that can facilitate reactions while reducing the amount of the solvent used during the reaction.[30–33] Their applications have been shown to outperform solution-based processes in terms of facilitating reactions, changing product composition, allowing lower reaction temperatures, reducing reaction times and improving sustainability indicators.[34–36] Other advantages of the method are its speed, reproducibility and simplicity, with considerable potential for extension to the design of a wide range of structures.[37,38]

Thus, in this work, we describe for the first time the synthesis of Zn bionanohybrids using a mechanochemical method, evaluating the experimental conditions to control the species and the structures generated to enhance the enzyme-like activities of the catalysts synthesized in the aqueous medium (Fig. 1).

Experimental part

Chemicals

p-Nitrophenylpropionate (*p*NPP) was obtained from Alfa Aesar (MA, USA). Sodium phosphate, sodium bicarbonate, zinc sulfate heptahydrate ($ZnSO_4 \cdot 7H_2O$) and *p*-aminophenol (*p*NP) were provided by Sigma-Aldrich (MA, USA). *Candida antarctica* lipase B (CALB) was from Novozymes (Bagsvaerd, Denmark). Hydrogen peroxide (33% v/v) and sodium hydroxide were obtained from Panreac (Barcelona, Spain). ABS (Acrylonitrile–Butadiene–Styrene) plastic and stainless-steel balls were obtained from RGPBalls (Italy).

Characterization methods

Spectrophotometric analyses were performed on a V-730 spectrophotometer. (JASCO, Tokyo, Japan). Inductively coupled plasma-optical emission spectroscopy (ICP-OES) was performed on the solid material. 5 mg of the solid powder was treated with 6 mL of HCl (37% v/v) for digestion. Then, it was added with 9 mL of water, centrifuged, and the clear solution was analysed for Zn content. Inductively Coupled Plasma-Optical Emission Spectrometry (ICP-OES) was performed on an OPTIMA 2100 DV instrument (PerkinElmer, Waltham, MA, USA). X-ray diffraction (XRD) patterns were obtained using a PANalytical X'Pert Pro polycrystalline X-ray diffractometer with a D8 advance analysis texture configuration (Bruker, Billerica, MA) with Cu Kα radiation ($\lambda = 1.5406$ Å, 45 kV, 40 mA). X'Pert Data Viewer and X'Pert Highscore Plus software were used for their analysis. Zn nanoparticle sizes and morphology were determined by transmission electron microscopy (TEM). Images were obtained using a S/TEM Titan 80–300 microscope equipped with a Cetcor Cs probe corrector and energy dispersion X-ray spectrometer (EDS) for chemical composition analysis. Samples for TEM observation were prepared by dispersing a small amount of the material in ethanol and putting a droplet of the suspension on a microscope copper grid covered with carbon film and allowing the alcohol to evaporate. Then, samples were dried and purified in a plasma cleaner. TEM (Bright Field BF, Dark Field DF, and Selected Area Diffraction) and STEM modes (BF detector to show the structure and morphology; and High Angle Angular Dark Field HAADF detector to reveal chemical contrast (Z-contrast)) were used for imaging. Because the tested material was sensitive to the electron beam, during microscopic observations, the intensity of the electron beam and the exposure time were limited.

General synthesis of aqueous Zn-enzyme bionanohybrids

1.6 mL of the commercial CALB solution (10.36 mg mL^{-1} determined by Bradford assay) was added to 60 mL of 0.1 M sodium bicarbonate pH 10 or sodium or sodium phosphate pH 7 to give a final enzyme concentration of 0.3 mg mL^{-1}. The corresponding enzyme solution was poured into a 100 mL glass bottle containing a small magnetic bar stirrer. Then, 600 mg of $ZnSO_4 \cdot 7H_2O$ (10 mg mL^{-1}) was added to the protein solution and stirred at room temperature for 17 h. After the first 30 minutes of incubation, the solution became cloudy and the pH of the solution was measured, showing a decrease in the pH of 8 or 6, depending on the buffer used. After 17 h, the mixture was
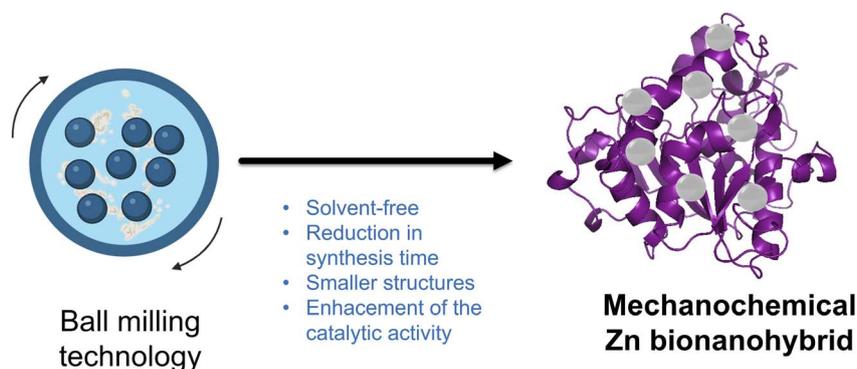

Fig. 1 Conceptual model of the mechanochemical synthesis of Zn bionanohybrids proposed in this work.

© 2024 The Author(s). Published by the Royal Society of Chemistry

centrifuged at 8000 rpm for 10 min and the recovered sediments were washed three times with distilled water (3 × 10 mL). Finally, the supernatant was removed and the pellet from each centrifuge tube was resuspended in 2 mL of water, collected in a cryotube, frozen in liquid nitrogen and lyophilised overnight. After that, the so-called Aq-Zn-BIC (0.323 g) and Aq-Zn-PHOS (0.071 g) were obtained.

Mechanochemical synthesis of Zn-BIC bionanohybrids

A 50 mL centrifuge tube was loaded with 600 mg $ZnSO_4$ and 500 mg sodium bicarbonate (pH 10) Then, 1.6 mL of CALB and 2 mL of distilled water were added to the solid powders as liquid-assisted grinding solvent (LAG). LAG was empirically characterized using the parameter η, based on how mechanochemical reactivity is affected by the ratio of the liquid additive to the weight of reactants ($\eta = V$ (liquid, $\mu L\ m^{-1}$ reagents, mg)). The values in LAG lie in the range of 0–2 $\mu L\ mg^{-1}$.[39] The mixture was ground using a planetary ball milling system with 10 g of 7 mm diameter stainless steel grinding balls (8 balls) at 45 rpm at 90° for 15 minutes. After the indicated time, the mixture was centrifuged at 8000 rpm for 10 min and the recovered sediment was washed three times with distilled water (3 × 10 mL). Finally, the supernatant was removed and the pellet from each centrifuge tube was re-suspended in 2 mL of water, collected in a cryotube, frozen in liquid nitrogen and lyophilised overnight. After that, the so-called M7-Zn-BIC, M7-Zn-BIC-2H₂O, M4.5-Zn–BIC and M4.5-Zn-BIC-2H₂O were obtained. M7-Zn-BIC-2H₂O-P catalyst was synthesised using the same protocol but by using 2 g of 7 mm plastic grinding balls (8 balls).

Mechanochemical synthesis Zn-PHOS bionanohybrids

A 50 mL centrifuge tube was loaded with 600 mg $ZnSO_4$, 588 mg $Na_2HPO_4 \cdot 2H_2O$ and 522 mg $NaH_2PO_4 \cdot 2H_2O$ (pH 7) (pH 7). Then, 1.6 mL of CALB and 2 mL of distilled water were added to the solid powders. The mixture was ground using a horizontal ball milling system with 10 g of 4.5 mm diameter stainless steel grinding balls (27 balls) at 70 rpm at 180° for 15 minutes. After the indicated time, the mixture was centrifuged at 8000 rpm for 10 min and the recovered sediment was washed three times with distilled water (3 × 10 mL). Finally, the supernatant was removed and the pellet from each centrifuge tube was re-suspended in 2 mL of water, collected in a cryotube, frozen in liquid nitrogen and lyophilised for 17 hours. After that, the so-called M-Zn-PHOS was obtained.

Esterase-like activity assay

The esterase-like activity of the Zn bionanohybrids was determined using the pNPP (p-nitrophenyl propionate) hydrolysis assay. This was performed by measuring the absorbance ($\lambda = 348$ nm) produced by the release of p-nitrophenol (pNP) upon hydrolysis of pNPP (50 mM) in sodium phosphate buffer (25 mM, pH 7). To initiate the reaction, 20 μL of pNPP standard solution (prepared in acetonitrile) was added to 2.5 mL of phosphate buffer. Then, 2 mg of the corresponding bionanohybrid was added under magnetic stirring. To determine the esterase-like activity for each bionanohybrid, the ΔAbs per min

value was calculated using the linear portion of the curve (ΔAbs). The specific activity (U per mg) was calculated using the following equation:

$$U \left(\mu mol\ min^{-1}\ mg^{-1} \right) = \Delta Abs/min \cdot V \cdot \frac{1000}{\varepsilon\ mg_{catalyst}}$$

where the molar extinction coefficient (ε) used was 43.6 $M^{-1}\ cm^{-1}$, and $mg_{catalyst}$ refers to mg of the hybrid metal.

Catalase-like activity assay

To start the reaction, 5 mg of the corresponding Zn bionanohybrid was added under gentle stirring to 2 mL of a 150 mM solution of H_2O_2 at room temperature. The degradation of hydrogen peroxide was then measured at 240 nm. An aliquot of the solution (0.2 mL) was taken at various times by diluting it in 2 mL of distilled water in quartz cuvettes of 1 cm path length. The specific activity (U per mg) was calculated using the previous equation.

Results and discussion

Mechanochemical Zn-BIC bionanohybrids

Aqueous Zn-BIC nanohybrids are known to have esterase-like activity. However, this catalytic activity is low. Therefore, in order to improve this result, the synthesis of the Zn hybrids was carried out mechanochemically.

Firstly, the preparation of aqueous zinc nanoparticle hybrids was attempted. 0.3 mg mL^{-1} of CALB (Fig. S1†) (commercial lipase B from *Candida antarctica*, 33 kDa, monomeric enzyme) dissolved in a basic medium (bicarbonate buffer at pH 10) was incubated with $ZnSO_4$ (10 mg mL^{-1}) for 17 h at room temperature. As a final step to obtaining the aqueous Zn bionanohybrid, a frozen suspension of the solid was lyophilised obtaining the hybrid called Aq-Zn-BIC (Fig. 2a).

Next, Zn bionanohybrids were synthesised mechanochemically (Fig. 2b). Different amounts of the solid powders (zinc salt and sodium bicarbonate) were first added in a centrifuge tube at complete dry conditions or the presence of a very small amount of water (2 mL), used as liquid-assisted grinding solvent (LAG) ($\eta = 1.81\ \mu L\ mg^{-1}$).

The mixture was ground using a planetary ball milling system with 10 g of 7 mm or 4.5 mm diameter stainless steel grinding balls at 45 rpm at 90° for 15 minutes. Experiments were also performed at longer incubation times (30 min), with fewer grinding balls (5 g). However, these variations did not lead to an improvement in the esterase-like activity (data not shown). After the indicated time, the solid was collected by centrifugation, washed with distilled water, frozen and lyophilised, obtaining the mechanochemical Zn bionanohybrids (Table S1†). Thus, the use of this method allows the amount of the solvent to be reduced (more than 30-fold) and the incubation time of the hybrid to be shortened (15 min *vs.* 17 h). In addition, when water is used as an additive, higher yields are obtained than when no water is used at all. Therefore, the use of water as LAG has a positive impact on the yield, with 2 mL being the optimal amount.
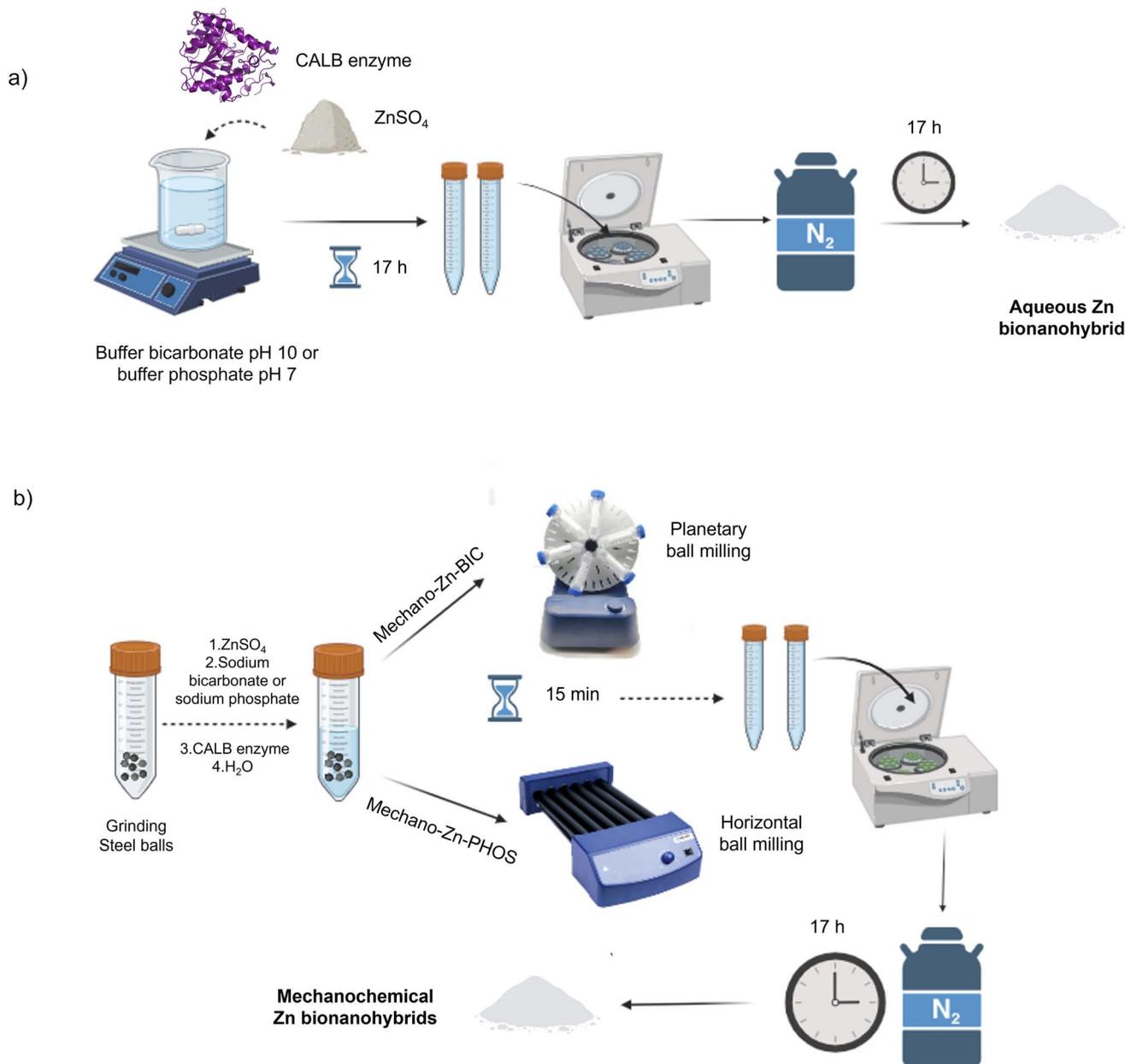
Fig. 2 Scheme for the synthesis of Zn bionanohybrids; (a) aqueous synthesis; (b) mechanochemical synthesis.

Next, wide-angle X-ray diffraction (XRD) was used to characterise the zinc structures generated in the biohybrids. The XRD pattern for Aq-Zn-BIC (Fig. S2†) showed peaks for 2θ at 31.8° (100), 34.5° (002) and 36.4° (101) corresponding to ZnO (JCPDS 36-1451).[40] The presence of this species was further confirmed by Fourier Transform Infrared Spectroscopy (FT-IR) (Fig. S3†), with the presence of the signature band of Zn–O symmetric stretching vibration at 457 cm^{-1} and 832 cm^{-1}, due to weak vibrations of ZnO.[41]

On the other hand, the X-ray diffraction patterns of mechanochemical Zn-BIC hybrids (Fig. 3a and S4–S6†) displayed characteristic peaks of $Zn_5(CO_3)_2(OH)_6$ at 31.8° (410) and 36.3° (021) (matched well with JCPDS 19-1458).[42] This was further confirmed from the FT-IR spectra (Fig. 3b and S7–S9†), with

a strong broad band centred at about 3317 cm^{-1} characteristic of the –OH stretching vibrations in $Zn_5(CO_3)_2(OH)_6$. The other peaks in the spectrum can be assigned to 1417 cm^{-1} and 1390 cm^{-1} (ν_3 mode of carbonate), 831 cm^{-1} (ν_2 mode of carbonate) and 710 cm^{-1} (ν_4 mode of carbonate) and the signature band of Zn–O symmetric stretching vibration at 457 cm^{-1}.[43] Mechanochemical synthesis is, therefore, able to induce a drastic change in the species present in the water-based counterpart hybrid.

Transmission electron microscopy (TEM) showed the formation of a cloud-like structure for the water-based bionanohybrid and HRTEM images revealed that the hybrid is actually a polycrystalline aggregate (Fig. S10†). For mechanochemical M7-Zn-BIC, the formation of slightly defined
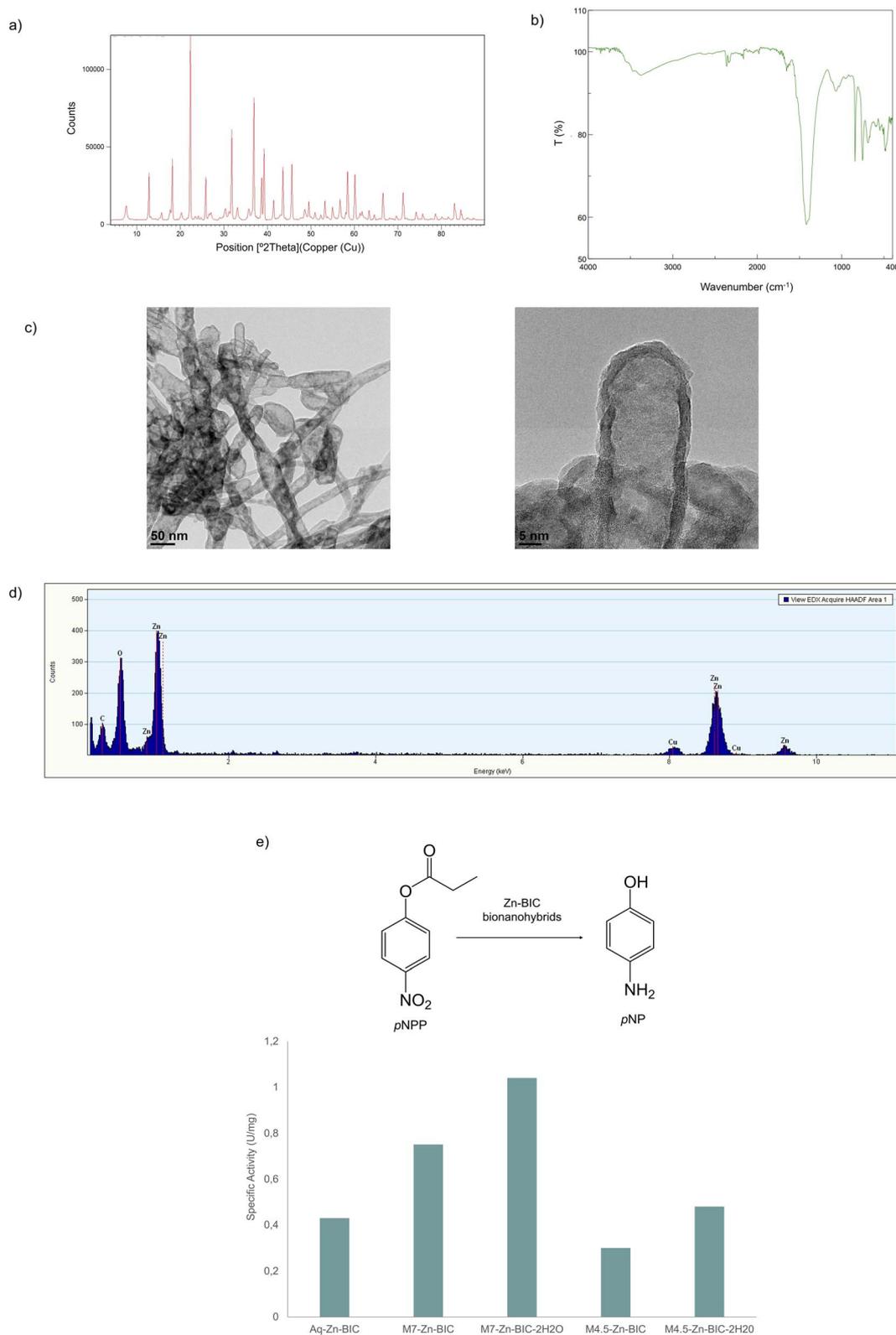
Fig. 3 (a) XRD pattern of M7-Zn-BIC-2H$_2$O. (b) FT-IR spectra of M7-Zn-BIC-2H$_2$O. (c) Transmission electron microscopy (TEM) and high-resolution TEM (HR-TEM) of M7-Zn-BIC-2H$_2$O. (d) STEM image of M7-Zn-BIC-2H$_2$O. (f) HAADF spectra of M7-Zn-BIC-2H$_2$O. (e) Esterase-like activity of the Zn-BIC bionanohybrids (r.t., aqueous media).

nanorods was observed (Fig. S11†). These nanorods become much more defined in M7-Zn-BIC-2H$_2$O with an average size of 500 × 30 nm (Fig. 3c). When using 4.5 mm grinding balls, M4.5-Zn-BIC (Fig. S12†) shows the formation of a crystalline aggregate similar to that observed with the water-based catalyst. However, analysis of M4.5-Zn-BIC-2H$_2$O (Fig. S13†) reveals channel-like structures of long length (200 × 30 nm). Therefore, when water is added as an additive, the nanostructure conformation of the aqueous catalyst can be drastically altered.

The chemical composition of the nanoparticles was determined by Annular Dark Field imaging (HAADF) (Fig. 3d). This technique indicates the presence of ZnO in the sample by showing the peaks for Zn and O in the water-based catalyst. (Fig. S14†). This technique, together with the DRX, FT-IR and X-ray diffraction techniques, showed the exclusive presence of Zn in the nanorods and the presence of the metal species Zn$_5$(CO$_3$)$_2$(OH)$_6$, with Zn, C and O peaks in the spectrum (Fig. 3e, S15 and S16†). Finally, the Zn content in the bionanohybrids

was determined by Inductively Coupled Plasma Optical Emission Spectroscopy (ICP-OES) analysis (Table S2†).

In the mechanochemical synthesis, the use of bicarbonate buffer in a non-aqueous media seems to produce coordination with Zn generating these species, confirmed by XRD and FT-IR. However, in the aqueous media, the presence of water leads to the coordination with the enzyme in a water molecules environment and the formation of ZnO as the main species, causing the buffer to exclusively control the pH and not for the coordination of Zn.

In order to verify that the metallic species are conserved when using materials other than stainless steel, the synthesis of M7-Zn-BIC-2H$_2$O was carried out with plastic beads, resulting in the so-called M7-Zn-BIC-2H$_2$O-P bionanohybrid. XRD patterns and FT-IR spectra (Fig. S17 and S18,† respectively) of this material match with those obtained using the stainless steel grinding balls. It is therefore the same metallic species: Zn$_5$(CO$_3$)$_2$(OH)$_6$. These results suggest that, in this case, the
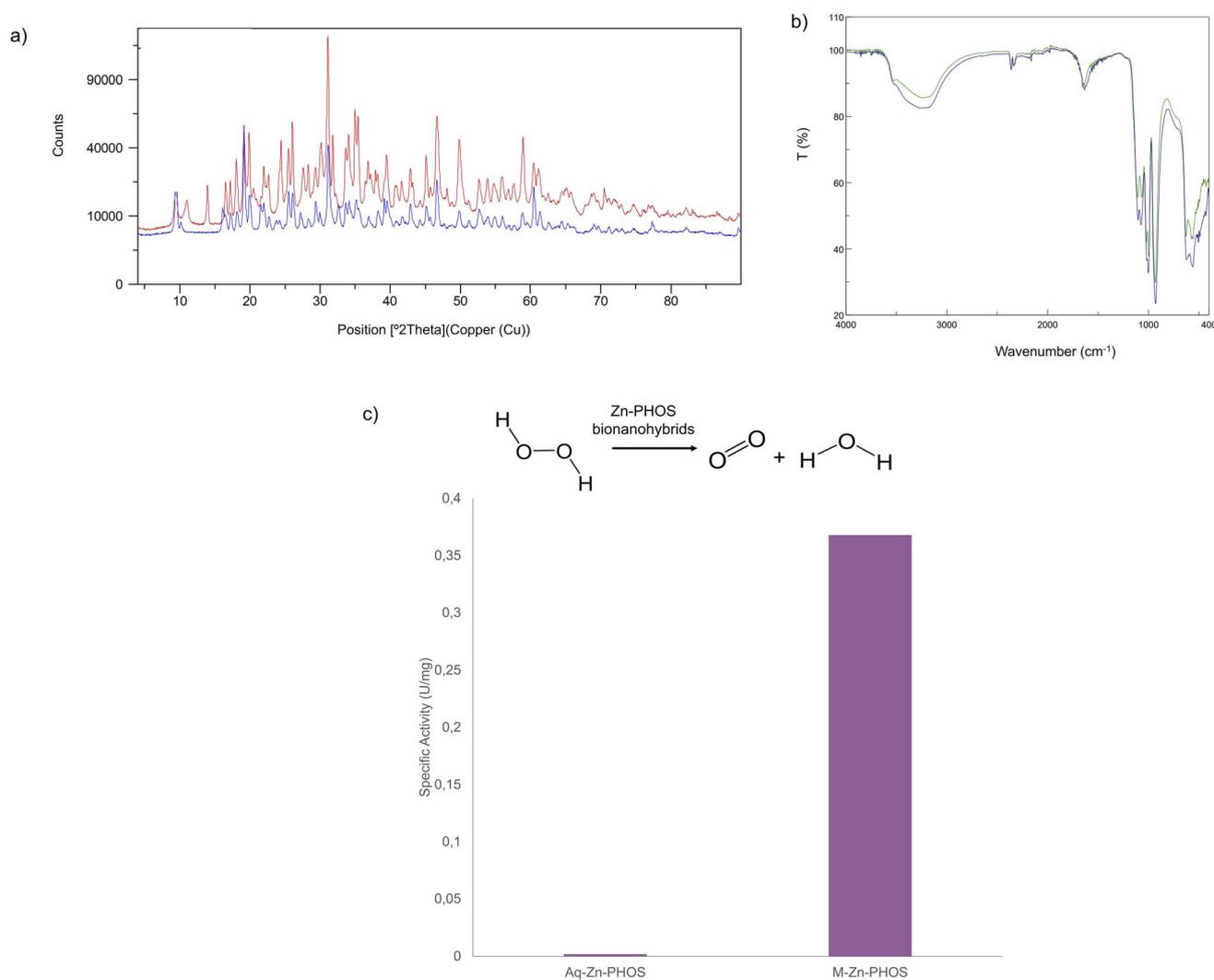

Fig. 4 (a) XRD pattern of Zn–PHOS bionanohybrids; blue line corresponds to Aq-Zn-PHOS and red line to M–Zn–PHOS. (b) FT-IR spectra of Zn–PHOS bionanohybrids. Blue line corresponds to Aq-Zn-PHOS and green line to M–Zn–PHOS. (c) Catalase-like activity of the Zn–PHOS bionanohybrids (r.t., aqueous media).

production of metal species was independent of the type of material used in mechanochemical synthesis.

The esterase-like activity of the mechanochemical Zn-BIC hybrid was then evaluated in the pNPP (p-nitrophenyl propionate) hydrolysis assay in aqueous media and room temperature (Fig. 3f). Aq-Zn-BIC presented a specific activity of 0.43 U per mg. However, when M7-Zn-BIC was used, this value increased to 0.75 U per mg, making it almost 2 times more active than the water-based catalyst. This value is tripled when using M7-Zn-BIC-2H$_2$O. On the other hand, the hybrids synthesised using 4.5 mm grinding balls showed the same activity as that of the aqueous catalyst. This can be correlated with its structure, as the hybrids synthesised with 7 mm grinding balls present nanorods, and they have been reported to have a higher catalytic activity than other structures.[44] These nanorods are more defined in M7-Zn-BIC-2H$_2$O, leading to a higher catalytic performance. On the other hand, M4.5-Zn-BIC has a similar structure to the aqueous catalyst, resulting in low esterase activity. In the case of M4.5-Zn-BIC-2H$_2$O, the channel-like structures reduce the surface area of the catalyst and result in a low level of catalytic activity.

Therefore, by using different mechanochemical methods, it is possible to modify the structure and species of the catalyst in aqueous media, enhancing the esterase-like activity of the Zn bionanohybrids.

Mechanochemical Zn-PHOS bionanohybrids

In a second approach, Zn-PHOS bionanohybrids were synthesised mechanochemically to enhance the catalase-like activity of the water-based catalyst.

The preparation of the aqueous zinc bionanohybrid was carried out in a neutral medium (phosphate buffer pH 7) using the same protocol as for the aqueous Zn-BIC catalyst, obtaining the hybrid called Aq-Zn-PHOS. Then, the Zn-PHOS hybrid was synthesised mechanochemically. In a first attempt, the synthesis was carried out under the same conditions as for M-Zn BIC (planetary ball milling, grinding balls 7 mm, 2 mL of water as liquid-assisted grinding solvent (LAG) (η = 1.17 µL mg^{-1}), 15 min), using a mixture of phosphate salts to obtain a neutral medium (pH 7). However, no improvement in catalase-like performance was observed under these conditions. (data not shown). Therefore, the mechanochemical method was changed to horizontal ball billing using 4.5 mm diameter stainless steel grinding balls, obtaining the so-called M-Zn-PHOS.

XRD analysis showed the same pattern for the aqueous and mechanochemical Zn–PHOS hybrids (Fig. 4a), displaying characteristic peaks for Zn$_3$(PO$_4$)$_2$ at 19.3° (040), 31.3° (241), 47.5° (521) and 61.1° (303) (JCPDS 33-1474).[46] This was confirmed by FT-IR (Fig. 4b) with absorption bands at 1106 cm^{-1} and 1071 cm^{-1} corresponding to the anti-symmetric stretching and symmetric stretching of PO$_4^{-3}$. The P–O bending vibration bands at 931, 630 and 566 cm^{-1} were also observed. The band at 1640 cm^{-1} corresponds to the C=O stretching vibrations of the carboxyl groups in the protein and the broad band at 3262 cm^{-1} can be assigned to the –OH stretching vibration, indicating the
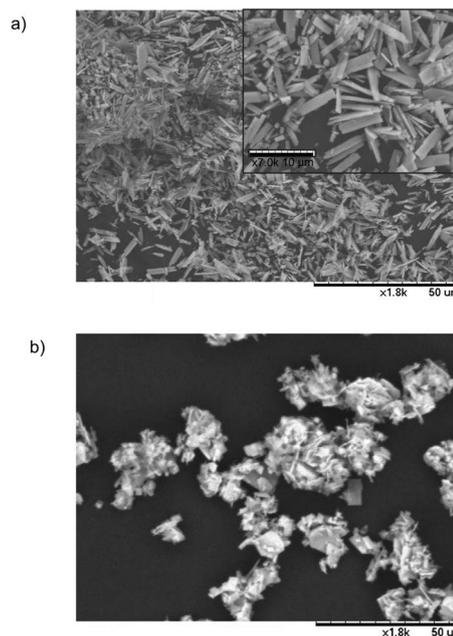

Fig. 5 Scanning electron microscopy (SEM) images of (a) Aq-Zn-PHOS and (b) M-Zn-PHOS.

presence of water in the protein.[45] Therefore, the chemical species is maintained using this methodology. ICP-OES analysis showed that the Zn content in the water-based bionanohybrid was 53% whereas for the mechanochemical was 33% (Table S2†).

The catalase-like activity of the mechanochemical Zn-PHOS hybrid was then evaluated in aqueous media and at room temperature (Fig. 4c). The specific activity of the Aq-Zn-PHOS bionanohybrid was 0.002 U per mg. However, this value increases up to 0.35 U per mg when the mechanochemically synthesised catalyst was used, making it 2000 times more active than the aqueous one.

Scanning electron microscope (SEM) analysis revealed the formation of crystalline Zn microplates for Aq-Zn-PHOS and Mechano-Zn-PHOS (Fig. 5). In the water-based catalyst, these microplates have an average size of 50 × 10 µm, whereas in the mechanochemically synthesised hybrid, the average size was significantly smaller, 12 × 6 µm. The structure of the nanohybrid can therefore be reduced by using mechanochemistry. This increase in catalase activity can be correlated with its structure as it has been observed that the mechanochemical hybrid has a smaller average size of microplates, resulting in a very large improvement of the catalytic performance.[46] This result again indicates that the synthesis of bionanohybrids in a mechanochemical way is able to induce drastic changes in the nanostructure of the water-based counterpart by increasing the catalase-like activity.

Conclusions

In this work, a procedure for the successful mechanochemical synthesis of novel Zn bionanohybrids was developed by the ball milling method. In the case of Zn-BIC hybrids, this technique

allowed changing of metal species from ZnO (in the aqueous catalyst) to $Zn_5(CO_3)_2(OH)_6$, as well as the structure (from cloud-like (in aqueous catalysts) to nanorods). For the Zn-PHOS hybrids, a significant reduction in structure was achieved, resulting in smaller microplates. Therefore, compared to the aqueous method, the mechanical approach induces changes in metal species and drastic changes in nanostructure conformation. In addition, the use of this technique resulted in a very large improvement in their catalytic performance, with the enzyme-like activity of the water-based catalysts being in some cases 2000 times more active than the water-synthesized counterpart. Together with this, the mechanochemical approach also allowed to synthesize these hybrids in a very short time (15 min *vs.* 17 h) without the necessity of a solvent.

Author contributions

J. M. P. conceived the project. J. M. P. supervised the project and obtained funding. C. G-S and L. G performed Zn bionanohybrids synthesis, characterization, and catalytic reactions. M. P performed bionanohybrids TEM characterization. J. M. P and C. G-S. analysed the data and wrote the manuscript.

Conflicts of interest

The authors declare no conflict of interest.

Acknowledgements

References

1 Y. Hu, J. O. Jensen, W. Zhang, L. N. Cleemann, W. Xing, N. J. Bjerrum and Q. Li, *Angew. Chem., Int. Ed.*, 2014, **53**, 3675–3679.

2 P. L. Saldanha, V. Lesnyak and L. Manna, *Nano Today*, 2017, **12**, 46–63.

3 Y. Wang, F. Wang, Y. Shen, Q. He and S. Guo, *Mater. Horiz.*, 2018, **5**, 184.

4 M. Filice, M. Marciello, M. D. P. Morales and J. M. Palomo, *Chem. Commun.*, 2013, **49**, 6876–6878.

5 D. Lopez-Tejedor, R. Benavente and J. M. Palomo, *Catal. Sci. Technol.*, 2018, **8**, 1754–1776.

6 N. Losada-García, A. Rodríguez-Otero and J. M. Palomo, *Catal. Sci. Technol.*, 2020, **10**, 196–206.

7 R. Benavente, D. Lopez-Tejedor, M. Del Puerto Morales, C. Perez-Rizquez and J. M. Palomo, *Nanoscale*, 2020, **12**, 12917–12927.

8 A. B. Moghaddam, F. Namvar, M. Moniri, P. Md Tahir, S. Azizi and R. Mohamad, *Molecules*, 2015, **20**, 16540–16565.

9 N. J. S. Costa and L. M. Rossi, *Nanoscale*, 2012, **4**, 5826–5834.

10 J. M. Palomo, *Chem. Commun.*, 2019, **55**, 9583–9589.

11 S. K. Das, M. R. Khan, A. K. Guhab and N. Naskar, *Green Chem.*, 2013, **15**, 2548–2557.

12 Z. Zhou, G. J. Bedwell, R. Li, P. E. Prevelige and A. Gupta, *Sci. Rep.*, 2014, **4**, 3832.

13 E. Enthaler, *ACS Catal.*, 2013, **2**, 150–158.

14 X. F. Wu and H. Neumann, *Adv. Synth. Catal.*, 2012, **354**, 3141–3160.

15 M. Mannarsamy, M. Nandeshwar, G. Muduli and G. Prabusankar, *Chem.–Asian J.*, 2022, **17**, e202200594.

16 Y. Yamashita, K. Minami, Y. Saito and S. Kobayashi, *Chem.–Asian J.*, 2016, **11**, 2372–2376.

17 N. U. Kumar, B. S. Reddy, V. P. Reddy and B. Rakeshwar, *Tetrahedron Lett.*, 2014, **55**, 910–912.

18 T. Onhisma, T. Iwasaki, Y. Maewaga, A. Yoshiyama and K. Mashima, *J. Am. Chem. Soc.*, 2008, **130**(10), 2944–2945.

19 D. Gao, Y. Zhi, L. Cao, L. Zhao, J. Gao, C. Xu, M. Ma and P. Hao, *J. Chem. Eng.*, 2022, **43**, 124–134.

20 R. Tayebee, A. H. Nars, S. Rabiee and E. Adibi, *Ind. Eng. Chem. Res.*, 2013, **52**(28), 9538–9543.

21 O. Saber, A. Osama, A. Alshoaibi, N. M. Shaalan and D. Osama, *Nanomaterials*, 2022, **12**, 2005.

22 M. I. Mahrsi, B. Chouchene, T. Gries, V. Carré, E. Girot, G. Medjahdi, F. Ayari, L. Balan and R. Schneider, *Colloids Surf. A: Physicochem.*, 2023, **671**, 131643.

23 T. H. Wei, S. H. Wu, Y. D. Huang, W. S. lo, B. P. Williams, S. Y. Chen, H. C. Yang, Y. S. Hsu, Z. Y. Lin, X. H. Chen, P. E. Kuo, L. Y. Chou, C. K. Tsung and F. K. Shieh, *Nat. Commun.*, 2019, **10**, 5002.

24 S. L. James, C. J. Adams, C. Bolm, D. Braga, P. Collier, T. Friščič, F. Grepioni, K. D. M. Harris, G. Hyett, W. Jones, A. Krebs, J. Mack, L. Maini, A. G. Orpen, I. P. Parkin, W. C. Shearouse, J. W. Steed and D. C. Waddell, *Chem. Soc. Rev.*, 2012, **41**, 413–447.

25 L. Takacs, *Chem. Soc. Rev.*, 2013, **42**, 7649–7659.

26 T. Friščič and W. Jones, *Cryst. Growth Des.*, 2009, **9**, 1621–1637.

27 K. Uzarevič, I. Halasz and T. Friščič, *J. Phys. Chem. Lett.*, 2015, **6**, 4129–4140.

28 T. Friščič, *Chem. Soc. Rev.*, 2012, **41**, 3493–3510.

29 F. Gomollón-Bell, *Chem. Int.*, 2019, **41**, 12–17.

30 T. Friščič, C. Mottillo and H. M. Titi, *Angew. Chem., Int. Ed.*, 2020, **59**, 1018–1029.

31 D. Tan and F. García, *Chem. Soc. Rev.*, 2019, **48**, 2274–2292.

32 J. Howard, Q. Cao and D. L. Browne, *Chem. Sci.*, 2018, **9**, 3080–3094.

33 N. R. Rightmire and T. P. Hanusa, *Dalton Trans.*, 2016, **45**, 2352–2362.

34 I. d'Anciaes, A. Silva, E. Bartalucci, C. Bolm and T. Wiegand, *Adv. Mater.*, 2023, **35**, 2304092.

35 E. Juaristi and C. G. Avila-Ortiz, *Synthesis*, 2023, **55**, 2439–2459.

36 M. T. J. Williams, L. C. Morril and D. L. Browne, *ChemSusChem*, 2022, **15**, e202102157.

37 F. Palazon, Y. El Ajjouri and H. J. Bolink, *Adv. Energy Mater.*, 2020, **10**, 1902499.

38 A. D. Jodlowski, A. Yépez, R. Luque, L. Camacho and G. de Miguel, *Angew. Chem., Int. Ed.*, 2016, **55**, 14972–14977.

39 P. Ying, J. Yu and W. Su, *Adv. Synth. Catal.*, 2021, **563**, 1246–1271.

40 S. Yedukar, C. Maurya and P. Mshanwar, *Open J. Synth. Theory Appl.*, 2016, **5**, 1–14.

41 G. Hitkari, S. Singh and G. Pandey, *Nano-Struct.*, 2017, **12**, 1–9.

42 M. Xiao, Y. Li, B. Zhang, G. Sung and Z. Zhang, *Nanomaterials*, 2019, **9**, 1507.

43 N. Kanari, D. Mishra, I. Gaballah and B. Dupré, *Thermochimica*, 2004, **410**, 93–100.

44 K. Zhou, X. Wang, X. Sum, Q. Peng and Y. Li, *J. Catal.*, 2005, **229**, 206–212.

45 J. D. Wang, D. Li, J. K. Liu, X. H. Yang, J. L. He and Y. Lu, *Soft Nanosci. Lett.*, 2011, **1**, 81–85.

46 D. P. Zulkifli and M. H. Kim, *CrystEngComm*, 2022, **24**, 4454–4464.